NANOPARTICLE

Research Article

Sequential Separation of U(VI) and Th(IV) by a Cyanex-921-Based Amberlite XAD-4 Chelating Resin

*Soaad Mohamed Elashry, Fatma S Hassen, A. I. L. Abd El Fatah**

Nuclear Materials Authority, 530-El Maadi Cairo, Egypt

Corresponding author:

A. I. L. Abd El Fatah

Nuclear Materials Authority, 530-El Maadi Cairo, Egypt,
Tel.: +20-1227020239,
E-mail: nuclic_science@yahoo.com

Received : July 12, 2025
Published : August 30, 2025

ABSTRACT

In this study, The incorporation of Cyanex 921 onto an XAD-4 polymeric support for selective separation and extraction of U(VI) and Th(IV) from aqueous solutions of natural sediment ore samples. It was shown that from an acidic solution, the successful loading of Cyanex 921 onto XAD-4 matrix was confirmed by FTIR and SEM. A batch sorption technique was used to examine the adsorption mechanism. Examined were pH, contact time, and adsorbent dose. The experimental results demonstrated that optimal loading capacities were achieved at a pH of 4 with 60 minutes of stirring for uranium, and at a pH of 3 with 30 minutes of stirring for thorium. The Langmuir and Freundlich isotherm models were utilized to mathematically represent the equilibrium data at room temperature, specifically at 25 °C. The maximum adsorption capacities of the impregnated resin for uranium (VI) and thorium (IV) were found to be 333.3 mg/g and 434.7 mg/g, respectively, per the Langmuir model at 25 °C. Chemical adsorption constituted the rate-limiting step in the adsorption of uranium and thorium onto the specified resin, adhering to the model of pseudo-second-order kinetics. The thermodynamic characteristics suggest that the process of adsorption of uranium and thorium onto impregnated Amberlite XAD-4 resin is marked by exothermically ($\Delta H < 0$) and spontaneity ($\Delta G < 0$). The impregnated resin demonstrates significant durability, and rapid equilibration. The described procedure has been accomplished implemented on actual sediment rock samples, indicating that the impregnated resin is an effective material for the extraction and recovery of U and Th ions derived from watery solutions.

Keywords: Impregnation, Sorption, Uranium (VI), Thorium (IV), XAD-4, Cyanex 921, Preconcentration

INTRODUCTION

Among heavy metals, considering their radioactivity and toxicity, uranium and thorium are undoubtedly the most dangerous to the environment. The strategic issue of chemists

DOI: https://doi.org/10.35702/nano.10020

ISSN: 2767-0171

is the exploration and mining, besides the processing, of ore materials that contain nuclear elements such as uranium and thorium, which represents the cornerstone of (industrial) nuclear technology [1-3]. Uranium and thorium find extensive application as nuclear fuel in power, and their main sources are pitchblende, monazite sand and sea water. Both metal ions are known to cause acute toxicological effects in mammals, and their compounds are potential occupational carcinogens [2]. Their recovery is essential to minimize their discharge into the environment from the point of view of safety and economy. Their selective extraction, simultaneously in the presence of each other and closely associated metal ions, has drawn much attention from chemists the world over because of their importance in energy-related applications [1]. Thus, there remains a need for pre-organized complexing agents that discriminate U(VI) and Th(IV) from associated metal ions present in great excess in solid or aqueous media [4]. The solvent extraction technique has been serving this purpose for many decades. Solid-phase extraction (SPE) has been increasingly used for the pre-concentration /separation of trace and ultra-trace amounts of inorganic and organic species from complex matrices, as seen from recent reviews [5,6]. Chelating resins have been frequently used as SPEs as they provide good stability, a high sorption capacity for metal ions and good flexibility in working conditions. Impregnated resins, which are designed by physically loading the successful organic extractants on a solid inert support material, have also been found to be effective for this process [7]. Chelating resins that are employed include Amberlite XAD series resins, 4-vinyl pyridine-divinylbenzene/acrylonitrile-divinylbenzene copolymers, Amberlite IRA-400, Biorad AGMP-1, silica-based C18 support, Amberlyst A-26, Dowex-2 and Merrifield chloromethylated resins. Amberlite XAD series resins have shown promise for designing chelating resins. There are two methodologies frequently adopted for designing such chelate-functionalized Amberlite XAD resins. The first involves the physical sorption of ligands onto a matrix. The other is based on covalent coupling of a ligand with a polymer backbone through a spacer arm, generally a –N=N– or –CH2 group [8]. The latter strategy renders rugged systems, free from ligand leaching problems, but their sorption capacities are low. One way of achieving high sorption capacity is by the use of ligands of small size which can extensively functionalize an appropriate crosslinked polymer. Several previous studies have been reported for the XAD series resins in which an inert support is impregnated or functionalized with a selective organic extractant, e.g., bicine [9], quinoline-8-ol [10] o-phenylene dioxydiacetic acid [11], tiron [12], Octa-O-methoxy resorcin [2] arene [13], Chrome Azurol S [14], succinic acid [15], o-aminobenzoic acid [16], N,N-dibutyl-N′-benzoylthiourea [17], Pyrogallol [18], alizarin red-s [19] and Octa-O-methoxy resorcin arene [2], to produce a solid sorbent for the isolation of U(VI) and/or Th(IV) from various analytical matrices.

The aim of this work was to synthesize a chelating resin by binding Cyanex 921 to Amberlite XAD-4 through a –CLN– group, and to study the adsorption and preconcentration of uranium and thorium from a sulfate solution. The experiments were carried out in a batch system. The influence of different variables such as pH, contact time and adsorbent dosage on the adsorption capacity of Amberlite XAD-4 resin impregnated with Cyanex 921 was investigated; the thermodynamic parameters of uranium (VI) and thorium (IV) adsorption were calculated at five different temperatures. Kinetic studies were performed in which the parameters were determined at 25 °C. Finally, the optimized factors were carried out for uranium (VI) and thorium (VI) recovery from sedimentary carbonaceous sandstone solution (real case).

EXPERIMENTAL

Instrumentation

The surface morphology of Amberlite XAD-4 resin impregnated with Cyanex 921 was studied by using a JEOL-JSM-5600LV scanning electron microscope model. UV–Vis spectrophotometer (SP-8001 UV-, Metretech Inc. version 1.02) that contains a glass cell of 10 mm. An atomic absorption model, G.B.C.A.A, was employed to measure trace elements in sulfate leach liquor. A UV-1 601 model Shimadzu UV–Vis spectrophotometer was used to determine U(VI) in a U(VI)–arsenazo(III) complex at 655 nm and Th(IV) in a Th(IV)–arsenazo(III) complex at 650 nm using arsenazo III as an indicator. Batch experiments were carried out in an isothermal circulator (Lindberg Blue, USA) at 200 rpm. The pH measurements were made with a Ino LabWTW model digital pH meter.

Chemicals and Reagents

High-purity reagents from Sigma-Aldrich, Merck and Fluka were used in the preparations of all standard solutions. Arsenazo III and Cyanex 921 (1% in kerosene) were purchased from Merck (Darmstadt, Germany). Standard and stock solutions were prepared using double-distilled water. On the other hand,

ISSN: 2767-0171

Amberlite XAD-4 (styrene divinyl benzene copolymer) with a surface area of 750 m^2 g^{-1}, a pore diameter of 50 Å and a bead size of 20–50 mesh was procured from Rohm and Hass Co., Collegeville, PA, USA. To remove inorganic and organic contaminants, it was washed with methanol, water, 1 mol L^{-1} HNO_3, water, 1 mol L^{-1} NaOH and water, respectively. For pH adjustment, 0.01 M H_2SO_4 and 1 M NaOH solutions were used.

Impregnation Process

The impregnation process was carried out by the dry method, which is the most widely used [20]. Of the dry Amberlite XAD-4 resin, 0.5 g was placed in 25 mL of kerosene containing 0.2 mmol of Cyanex 921 and stirred for 12 h. The resin was separated by filtration through a filter paper and was washed with double distilled water to remove the solvent. Then, the resin was dried at 70 °C and used as an air-dried product. The ligand content in the impregnated solution was determined gravimetrically by weighing. The amount of impregnated resin was calculated from the material balance to be 0.523 gm [21].

Batch Adsorption Experiments

The batch mode worked to optimize the equilibrium adsorption states of U(VI) and Th(IV) at various parameters, such as influence of pH, initial uranium and thorium concentration, contact time and temperature. In the experiments, 0.01 g of impregnated resin was equilibrated with 10 mL of solution containing 500 mg/L sulphate anion, and the flasks were then placed inside a mechanical shaker where the agitation speed was set at 200 rpm. The mixture was agitated for a specific time period at different temperatures. Hence, adsorbent and solution were separated by filtration through a filter paper. After each experiment, the concentration of uranium and thorium ions in the solution was determined by using a single-beam spectrophotometer, Meterch (SP-8001), using arsenazo III as an indicator at a wavelength of 655 nm.

Each experiment was carried out three times and the average results were reported. The relative standard deviation values of the results were relatively low and of the order of ± 2.5%, which shows the good reproducibility and accuracy of the experiments. The adsorption rate percentage, the adsorption capacity (qe, mg/g) and the distribution coefficient (Kd, mL/g) were calculated using the following equations:

$$R_e(\%) = [(C_i - C_e)/ C_i] \times 100 \quad (1)$$

$$q_e\ (mg/g) = (C_i - C_e) \times V/m \quad (2)$$

$$K_d\ (ml/g) = [C_i - C_e/ C_e] \times V/m \quad (3)$$

where C_i is initial concentration of the metal ion (mg/L), Ce is the equilibrium concentration of the metal ion after adsorption (mg/L), V is the volume of the metal ion aqueous solution contacted with adsorbent (L), and m is the amount of adsorbent (g).

RESULT AND DISCUSSION

Characterization of Materials

Energy-Dispersive X-Ray Spectroscopy (EDX)

Figure 1a shows the scanning electron microscope (SEM) images of the polymeric chelating resin modified with Cyanex 921. The composition of all the elements in modified resin differs from those present in its original form. This is due to the addition of Cyanex 921, which modifies the surface of XAD-4, leading to a decrease in the percentage of the present elements. The scanning electron microscope (SEM) images with the EDX spectra of the impregnated resin loaded with thorium and uranium are presented in Figure 1b, c, respectively.

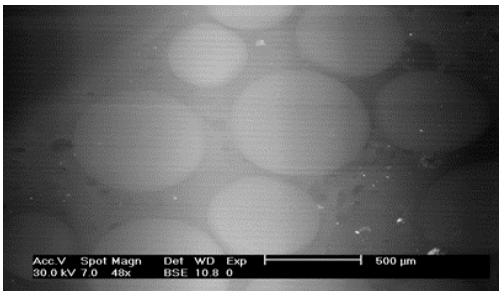

(**a**)

DOI: https://doi.org/10.35702/nano.10020

ISSN: 2767-0171

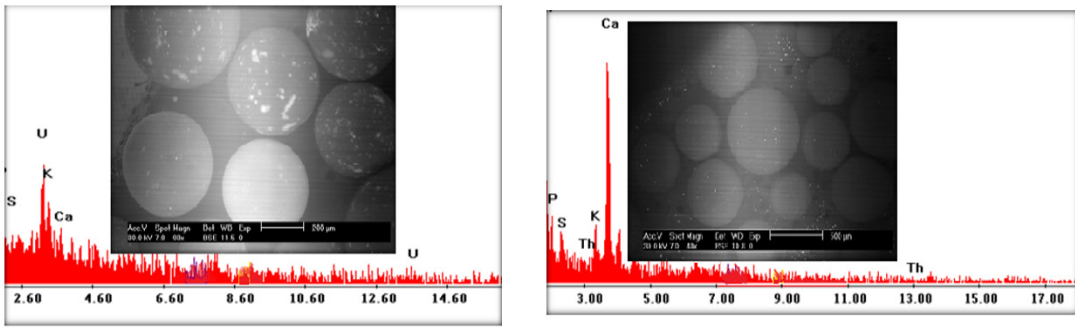

(b) (c)

Figure 1. SEM images and EDX for (**a**) the Cyanex-921-based Amberlite XAD-4 chelating resin, (**b**) the impregnated resin after uranium adsorption and (**c**) the impregnated resin after thorium adsorption.

Fourier-Transform Infrared Spectroscopy (FTIR) Investigation

FTIR is a vital analysis technique that reveals the various characteristic functional groups existing in the studied impregnated resin. The Fourier-transform infrared spectra (FTIR) of the Amberlite XAD-4 resin impregnated with Cyanex 921 and the impregnated resin loaded with uranium and thorium are given in Figure 2. From the latter, intense bands at 1131, 709.8, 794.6 and 902.6 cm^{-1} were observed. The broad band at 3147.8.10 cm^{-1} is due to symmetric and asymmetric—OH stretching, whereas the band at 1604.7 cm^{-1} is due to H-O-H bending. The C–H bending vibrations are visible at 632.6 cm^{-1}. The associated amine is represented by the band at 1543 cm^{-1}, and the peaks at 1543.05, 1666.49 and 1396.64 cm^{-1} could be attributed to the presence of C = O groups (carbonyl, carboxy and quinones). After thorium and uranium adsorption, the bands at 3140.11 and 3147.82 cm^{-1} were observed, respectively.

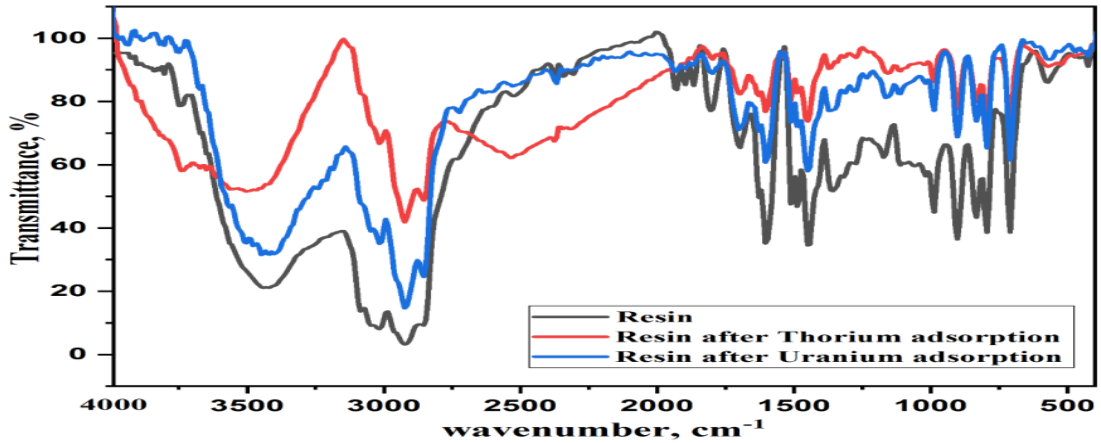

Figure 2. FTIR spectra of the Cyanex921-based Amberlite XAD-4 chelating resin as well as after thorium and uranium adsorption.

DOI: https://doi.org/10.35702/nano.10020

ISSN: 2767-0171

Sorption studies

Optimum pH of Metal Ions Uptake

The uranium (VI) and thorium (IV) adsorption efficiency of Cyanex-921-based Amberlite XAD-4 polymeric chelating resin was found to be strongly dependent on the variation in pH of the solution. Therefore, uranium (VI) and thorium (IV) adsorption experiments were carried out at different pH levels (1, 1.5, 2, 2.5, 3, 3.5, 4 and 4.5), under the conditions of the initial uranium and thorium content of 500 ppm, using 0.01 gm of impregnated resin and 10 mL of uranium and thorium solution, which was shaken for 180 min, at room temp. The results of uranium and thorium adsorption onto impregnated resin at different pH levels are illustrated in Figure 3.

As can be seen in Figure 3, the maximum uptake value is observed at a pH of 3 and 4 for Th and U, respectively. In an acidic solution and at pH levels less than 2, the predominant species seem to be $(UO_2)^{2+}$ ions. However, the presence of high contents of sulfate in the solution enhances the formation of complexes such as $UO_2(SO_4)^{2-}$ and $UO_2(SO_4)^{3-}$ [22]:

$$UO_2 + SO_4 \rightarrow UO_2(SO_4)\ K1 \quad (4)$$

$$UO_2(SO_4) + SO_4 \rightarrow UO_2(SO_4)_2^{2-}\ K2 \quad (5)$$

$$UO_2(SO_4)^{2-} + (SO_4)^{2-} \rightarrow UO_2(SO_4)_3^{4-}\ K3 \quad (6)$$

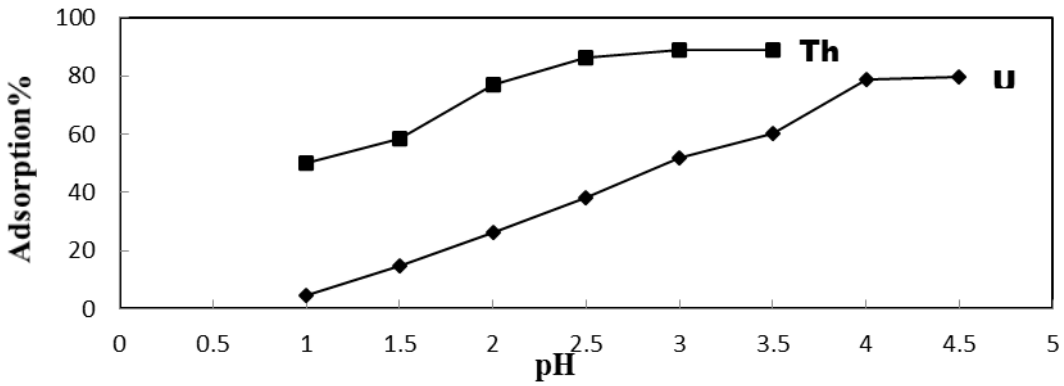

Figure 3. Effect of pH on the adsorption of uranium and thorium onto Cyanex-921-impregnated Amberlite XAD-4 resin.

Equations (4)–(6) indicate the equilibrium state between uranium and sulphate ions in the solution. The constants K1, K2 and K3 are called stability constants in a pH range of 3–4 as no significant change in the adsorption of uranium complexation was noticed. Increasing the pH level above 4.0 would lead to uranium precipitation, which is the reason why the experiments were not performed at values higher than 4 [23].

On the other hand, different chemical forms of Th(IV) can be possible in solutions with different pHs [24]. Th^{4+} is the least hydrolyzed tatrapositive ion; the un-complexed cation is stable at a pH of 3 or less. $Th(OH)^{3+}$ around a pH of 3–5, $Th(OH)^{2+}$ around a pH of 4.5–5.5, $Th(OH)^{3+}$ around a pH of 5 and $Th(OH)_4$ above a pH of 6 are formed [25]. In this work, $Th(OH)^{3+}$ and $Th(OH)^{2+}$ species may be dominant in the adsorption of thorium by Cyanex-921-impregnated resin.

The obtained results shown in Figure 3 indicate that, as the pH of the solution increases from 1 to 4.5 for uranium and from 1 to 3.5 for thorium, the adsorption uptake of metal ions was found to be increasing until reaching a steady state at a pH of 4.5 and 3.5 for U(VI) and Th(IV), respectively, with (q_e = 315.5 and 417.3). This may be due to variations in pH, which cause changes in adsorbed species in solutions, and precipitation begins due to the formation of complexes in the aqueous solution. Therefore, pH is adjusted to 4 and 3 pH for uranium and thorium, respectively, and this is the best pH. The studies revealed the selective extraction of metal ions at particular pH levels, thereby suggesting the possibility of the separation of metal ions in the presence of each other.

Effect of Adsorbent Dosage

The relationship between adsorbent dosage and adsorption efficiency has also been investigated. The volume of the

DOI: https://doi.org/10.35702/nano.10020

ISSN: 2767-0171

solution (10 mL), the concentration of uranium and thorium (500 g/L), the pH of the solution at 4 or 3 for U(VI) and Th(IV), respectively, and the time of adsorption (60 min) were kept constant, while the amount of resin varied from 0.01 to 0.1 g/L. As shown in Figure 4, by increasing the amount of adsorbent the adsorption percentage of uranium and thorium increases.

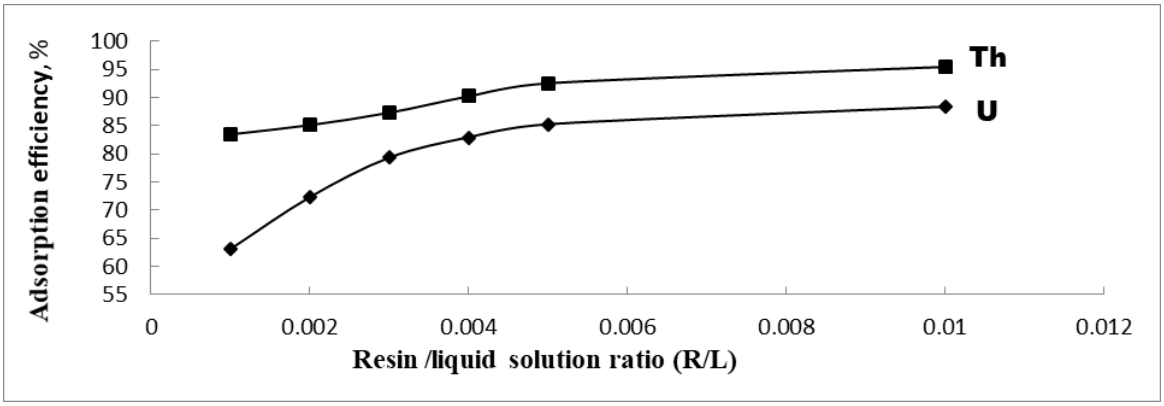

Figure 4. Effect of resin/liquid solution ratio on uranium and thorium adsorption.

The increase observed in adsorption due to increasing the amount of adsorbent could be attributed to the increase in surface area and the availability of adsorption sites [26]. While at a constant concentration, increasing adsorbent levels lead to more unsaturated sites, which could be the reason why the amount of uranium and thorium adsorption per unit weight of adsorbent decreases. Accordingly, the sorption efficiency of uranium and thorium were increased from 63.1 and 83.46 to 80.3 and 95.4%, respectively, by increasing the resin dose from 0.001 to 0.05 mg, and it has remained constant thereafter till 0.01 mg. The results show that the maximum uptake capacity of prepared impregnated resin is 401.5 and 477 mg/g for U (VI) and Th (IV), respectively.

Effect of Contact Time

The contact time is one of the major efficient factors in the adsorption process of ions. Figure 5 provides data on the effect of contact time on batch adsorption of uranium (VI) and thorium (IV) onto impregnated resin at different time intervals up to 180 min. In the present step, the experiments were conducted under optimum conditions and initial concentrations of uranium and thorium was (500 mg/L), respectively. From Figure 5, it can be observed that the uranium and thorium adsorption percentage grew rapidly by increasing contact time and then reached the saturation point in 60 min. After that, no significant change in the adsorption of uranium (IV) and thorium (IV) was noticed. It should be mentioned that the data obtained in this step were used for subsequent kinetic studies.

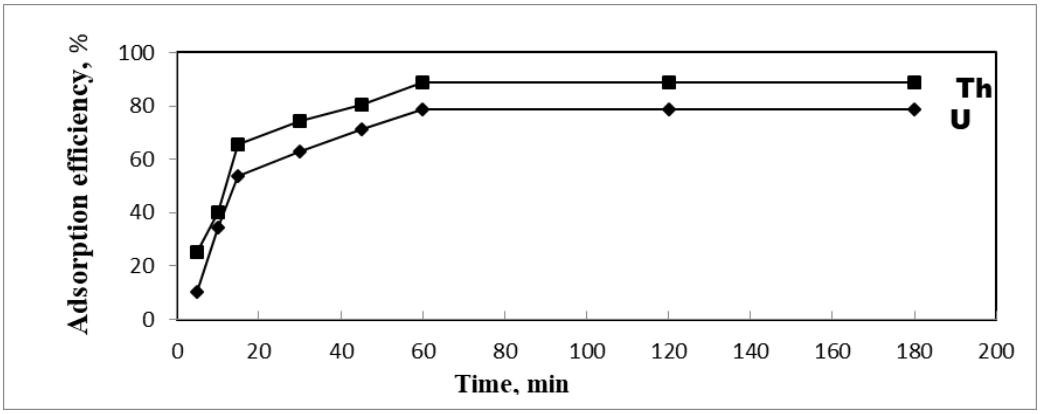

Figure 5. Effect of contact time on the adsorption of uranium and thorium onto impregnated resin.

ISSN: 2767-0171

Adsorption Kinetics Study

To determine the kinetics of uranium and thorium adsorption on impregnated resin, kinetics experimental data were simulated using pseudo-first-order and pseudo-second-order models. The linear form of the pseudo-first-order model can be represented by a simple Lagergren equation [27]:

$$\log(q_e-q_t)=\log(q_e)-K_1 t/2.303 \quad (7)$$

Where K_1 represents the pseudo-first-order adsorption rate constant, q_e (mg/g) is the adsorption capacity of uranium and thorium at equilibrium, t is the time (min) and q_t is the amount of adsorbed metal ions at the time, t (mg/g). K_1 could be obtained by plotting $\log(q_e-q_t)$ versus t (Figure 6).

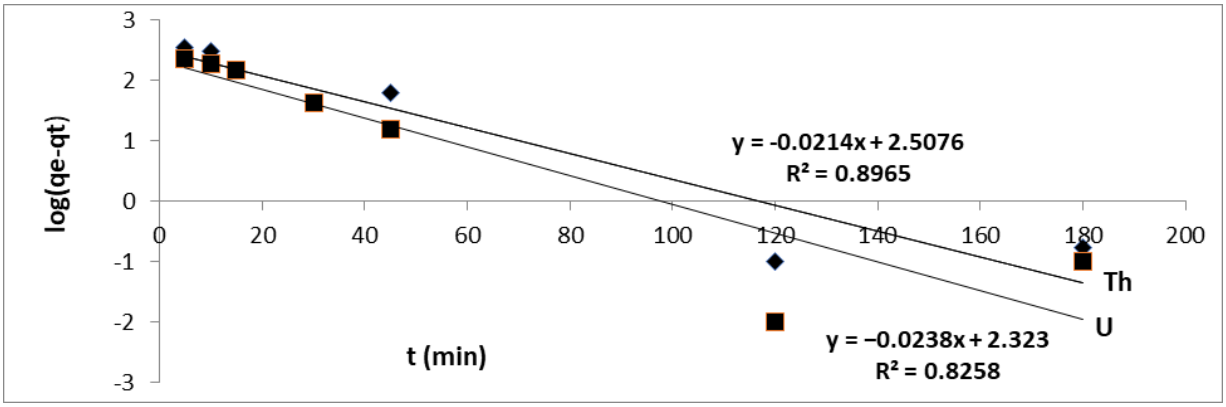

Figure 6. Pseudo-first-order kinetics of uranium (VI) and thorium (IV) adsorption onto impregnated resin.

The linear pseudo-second-order kinetic model could be shown as:

$$t/q_t=1/k_2q^2_e+ 1t/q_e \quad (8)$$

Where k_2 is the pseudo-second-order adsorption rate constant (g/mg min) [28]. K_2 can be determined from the slope of plot t/q_t versus t (Figure 7).

The parameter values of the pseudo-first-order and pseudo-second-order models at initial concentrations of uranium and thorium are presented in Table 1 and by comparison between it. The regression correlation coefficients (R^2) at initial concentrations of uranium and thorium for the pseudo-first-order model seem to be lower, and experimental qe does not agree with calculated qe. On the other hand, for the pseudo-second-order model the initial concentrations of uranium and thorium are closer to unity (0.9941 and 0.9667), and are higher than the obtained value using the pseudo-first-order model, and the qe (theoretical equilibrium adsorption capacity) for uranium and thorium shows good agreement with qe exp. (experimental equilibrium adsorption capacity). According to the comparison between the values of qe exp and qe calculated by the two models, it can be proved that the adsorption process of U and Th (IV) ions onto modified resin is governed by the pseudo-second-order model and controlled by chemical sorption, with the rate-limiting step in the process potentially being chemical adsorption [29].

The Elovich equation is often employed to clarify the adsorption kinetics and successfully demonstrate chemisorption on heterogeneous sorbents. The linear Equation (9) is reported by [30]:

$$Q_t = 2.303\beta\log(\alpha\beta) + 2.303\ \beta\log_t \quad (9)$$

Where *α* and *β* are Elovich coefficients that show the initial sorption rate (g mg^{-1} min^{-2}) and the desorption constant (mg g^{-1} min^{-1}). The relationship between q_t and log*t* for the removal of U(VI) and Th(VI) onto the prepared impregnated adsorbent material is demonstrated in Figure 8. The plots exhibit good linear relations from their slopes and intercepts, more so in the case of uranium than thorium. Elovich constants were determined and are given in Table 1. These values predicted that the Elovich model may comprise that the chemisorption of U(VI) and Th(IV) ions on our modified polymeric resin sorbent represent the rate of chemisorption of sorption *α*, and constant *β* refers to the exterior covered [30]. The Elovich equation is useful in describing the chemical sorption of heterogeneous systems [30].

DOI: https://doi.org/10.35702/nano.10020

ISSN: 2767-0171

Table 1. Kinetics parameters for the sorption of U(VI) and Th(IV) ions by different prepared impregnated resin

Element	Exp.q_e (mgg^{-1})	Pseudo-First-Order q_e (mg g^{-1}) K_1 (min^{-1}) R^2	Pseudo-Second-Order q_e (mgg^{-1}) $K2$ R² (g mg^{-1} min^{-1})	Elovich A β (mg g^{-1} min^{-1}) R² (g mg^{-1} min^{-2})
U(VI)	315.7	210.37	344.82	0.009
		0.054	0.0341	85.02
		0.8258	0.9941	0.9235
Th(IV)	417.3	321.36	479.16	0.0046
		0.049	0.00013	108.46
		0.896	0.9667	0.846

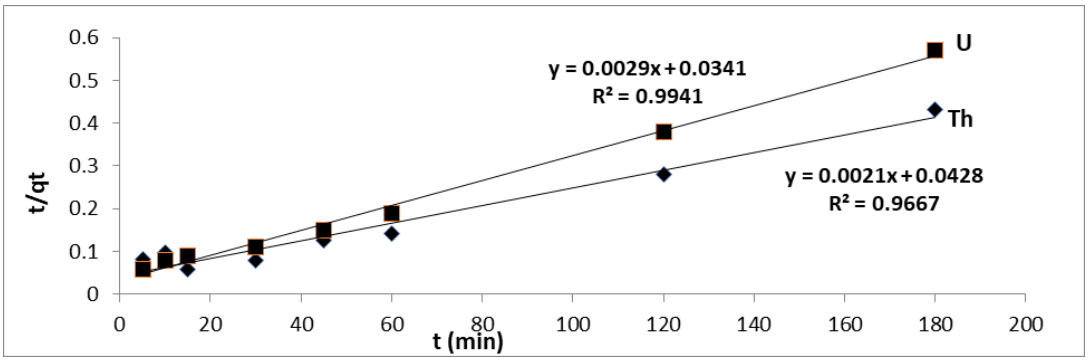

Figure 7. Pseudo-second-order kinetics of uranium (IV) and thorium (VI) adsorption onto impregnated resin.

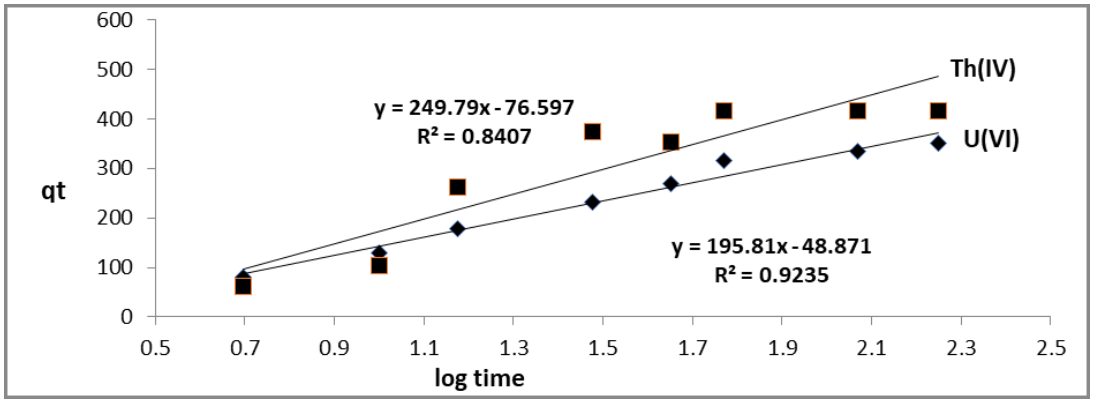

Figure 8. Elovich plots for sorption of uranium and thorium onto impregnated resin.

DOI: https://doi.org/10.35702/nano.10020

ISSN: 2767-0171

Adsorption Isotherm Study

Sorption isotherms are empirical models that describe the relationship between the equilibrium concentration of the adsorbate and the amount adsorbed on a solid surface at a constant temperature.

The sorption isotherms for U (VI) and Th (IV) removal were studied using initial concentrations ranging from 50–1000 mg L^{-1}, as given in Figure 9. The results revealed that the maximum capacity (qe) was 333.3 and 434.78 mgg^{-1} for U (VI) and Th (IV), respectively, using the adsorbent resin. In order to analyze the experimental equilibrium adsorption data in the present study, the Langmuir and Freundlich isotherm models were applied. The Langmuir adsorption isotherm assumes that adsorption takes place on a surface that is energetically homogeneous, and that there is no interaction between neighboring adsorbed molecules on the surface of the adsorbent [31], while the Freundlich model assumes that adsorption occurs on a heterogeneous surface [32]. The linear form of Langmuir and Freundlich isotherms are presented by Equations (10) and (11), respectively:

$$C_e/q_e = 1/bq_{max} + C_e/q_{max} \quad (10)$$

$$\ln q_e = \ln K_F + 1/n \ln C_e \quad (11)$$

Where C_e is the equilibrium concentration of uranium in the solution (mg/L), q_e is the amount of uranium adsorbed per weight unit of resin at equilibrium time (mg/g), q_{max} is the saturated monolayer adsorption capacity (mg/g) and b is the Langmuir constant (L/mg). K_F ((mg/g) (L/mg)1/n) and n are the Freundlich constants related to adsorption capacity and adsorption intensity, respectively.

The Langmuir and Freundlich plots are presented in Figures 9 and 10, respectively, and their parameters and regression correlation coefficients are given in Table 2.

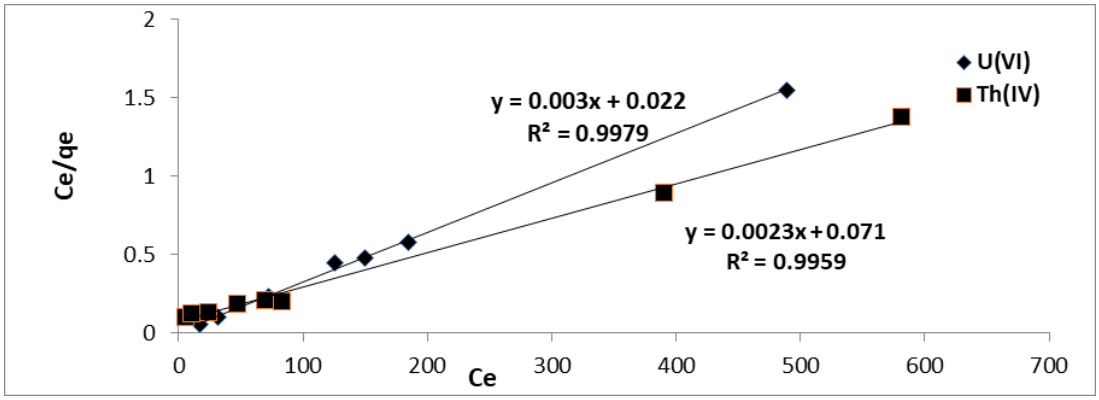

Figure 9. Langmuir adsorption isotherms for uranium (VI) and thorium (VI) adsorption onto impregnated resin at different concentrations.

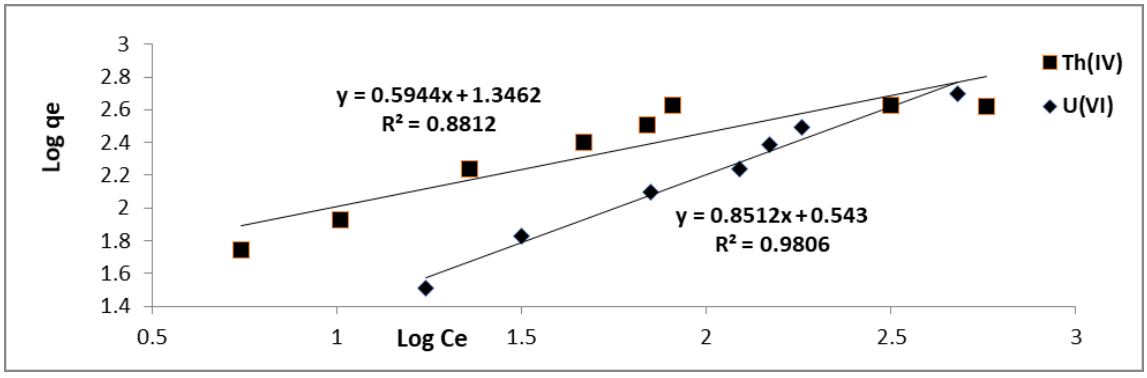

Figure 10. Freundlich adsorption isotherms for uranium (VI) and thorium (IV) adsorption onto impregnated resin.

DOI: https://doi.org/10.35702/nano.10020

ISSN: 2767-0171

Table 2. Langmuir and Freundlich isotherm constants uranium and thorium sorption onto the impregnated resin

Element	Langmuir Constants			Freundlich Constants		
	Q_{max} (mgg^{-1})	k_L ($L\ mg^{-1}$)	R^2	(k_F)	(n)	R^2
U	333.3	0.136	0.9976	3.491	1.203	0.9806
Th	434.78	0.032	0.9966	22.19	1.682	0.8812

As presented in Table 2, at room temperature the Langmuir model gave slightly better fittings than the Freundlich model. The maximum uranium and thorium adsorption capacity of the impregnated resin in the presence of the sulphate anion was 333.3 and 434.78 mg/g, respectively. Comparisons between maximum uptake capacities (q_m) of impregnated Amberlite XAD-4 and other adsorbents for uranium (VI) and thorium reported in the literature are presented in Table 3. It is revealed that sorbent materials are efficient and economical adsorbent materials.

The result shows that impregnated resin exhibits a reasonable capacity for uranium and thorium adsorption from aqueous solutions. Additionally, the values of n being larger than 1 shows the favorable nature of uranium and thorium adsorption onto impregnated Amberlite XAD resin. The essential characteristic parameter of the Langmuir isotherm that indicates the type of isotherm is the dimensionless factor R_L. Favorable adsorption will occur when the R_L value is in the range of 0–1 [33]. This parameter is defined by the following equation:

$$R_L=1/1+bC_i \quad (12)$$

where C_i is the initial uranium concentration (mg/L) and b is the Langmuir constant (L/mg). As shown in Table 3, R_L is greater than 0, which indicates that the adsorption of uranium onto the impregnated Amberlite XAD is favorable.

Table 3. The Calculated values of the equilibrium parameter, R_L, of the Langmuir model for uranium and thorium

Element	R_L,						
Conc. mg/L	50	100	200	300	400	500	1000
U	0.128	0.068	0.035	0.023	0.018	0.014.	0.007
Th	0.384	0.238	0.135	0.094	0.072	0.058	0.030

Finally, it is clear from Table 2 and Figure 9, that the parameters of the Langmuir isotherm model are closer to the experimental values than those fitted by other models.

Thermodynamics Study

For evaluating the effect of temperature on the adsorption of U (VI) and Th (IV) using synthesized resin, the adsorption process was conducted in a series of batch experiments under various temperatures ranging from 25 to 70 °C. The other parameters were as follows: a concentration of each uranium and thorium of 0.5 mg L^{-1}, an adsorbent amount of 0.01 g and a solution volume of 10 mL. As seen from Figure 11, heating in the examined range only slightly affects the adsorption.

DOI: https://doi.org/10.35702/nano.10020

ISSN: 2767-0171

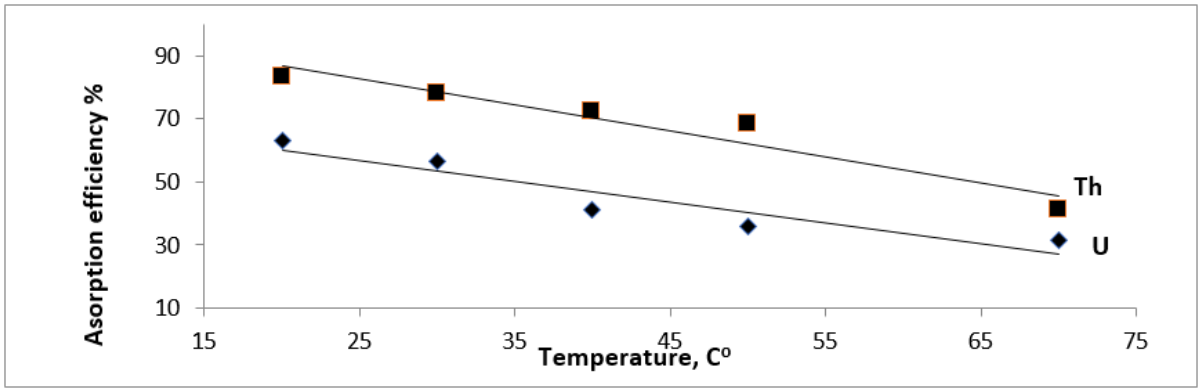

Figure 11. Effect of temperature on the adsorption efficiency of uranium and thorium using synthesized impregnated resin.

The standard free energy of adsorption (ΔG°) was determined using the following equation:

$$\Delta G^\circ = \Delta H^\circ - T\Delta S^\circ \quad (13)$$

Where, ΔH° is the enthalpy of adsorption, ΔS° is the entropy change and T is the temperature (K). From the slope and intercept of the Van't Hoff equation, which is shown in Equation (13), ΔH° and ΔS° can be calculated (Figure 12):

$$\log K_d = \Delta S^\circ/2.303R - \Delta H^\circ/2.303RT \quad (14)$$

Where R is the universal gas constant (8.314 J/mol K) and T is the absolute temperature (K).

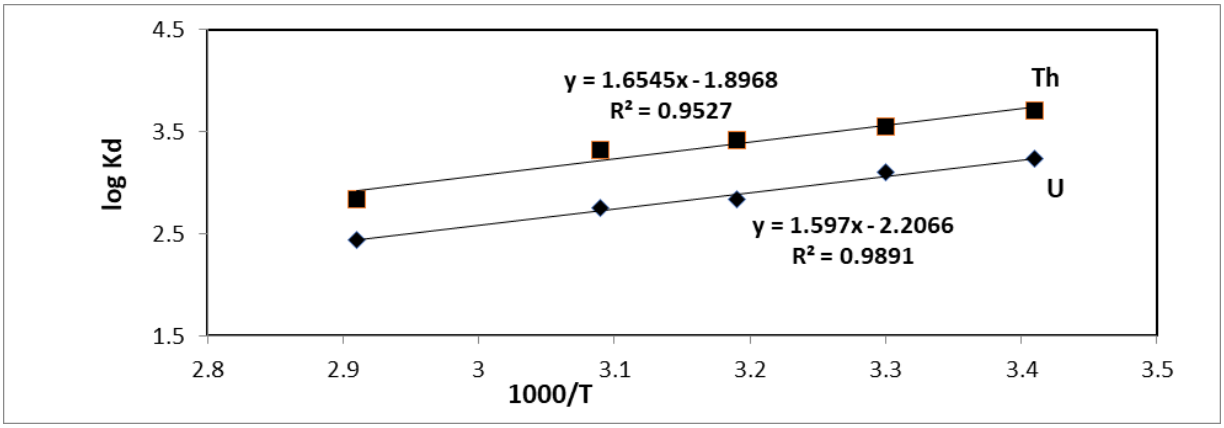

Figure 12. Plot of Log K_d versus 1000/T for uranium and thorium sorption onto impregnated resin.

The values of thermodynamics parameters are given in Table 4. The negative value of ΔH° indicates that the adsorption of uranium onto the impregnated resin is exothermic. In addition, the negative standard free energy and the negative standard entropy indicate that the adsorption reaction is a spontaneous process and is more unfavorable at higher temperatures.

DOI: https://doi.org/10.35702/nano.10020

ISSN: 2767-0171

Table 4. Thermodynamic parameters for uranium and thorium adsorption onto impregnated resin at 500 mg/L initial U (VI) and Th (IV) concentrations

Metal Ions	ΔH, KJ/mol	ΔS, KJ/mol.K^{-1}	ΔG, KJ/mol				
			293 K	303 K	313 K	323 K	343 K
U(VI)	−30.57	−0.042	−18.19	−17.79	−17.36	−16.96	−16.1
Th(IV)	−13.65	−0.036	−21.10	−20.74	−20.38	−20.02	−19.30

Comparative to Other Adsorbents

To get enhanced facts on the sorption characteristic of the prepared matrix as an efficient new adsorbent for U (VI) and Th (IV), the measured sorption capacity is compared with those of other sorbents. The q_e value for sorption for the nuclides on different materials are compared with a modified XAD-4 adsorbent, as summarized in Table 5. The results demonstrated that the prepared material is promising for the elimination and/or separation of U (VI) and Th (IV) from their solutions.

Table 5. Comparison of adsorption capacities of various adsorbents used for uranium and thorium adsorption

Adsorbent Sorption Capacity	References
Ambersep 400 ($SO4^{2-}$) 50 mg/g for U	[34]
Amberlite IRA 67 50 mg/g for U	[35]
Amberlite IRA-402 213 mg/g for U	[36]
Modified activated carbon with quinoline 63 mg/g for U	[37]
Chitosan/amine resin 481.1 mg/g for U	[38]
Lewatit mono plus M500 40.6 mg/g for U	[39]
Amberlite XAD-16 214.2 mg/g for U	[17]
Amberlite XAD-4 functionalized with bicine ligands Th 0.25 and U 0.38 mmol g^{-1}	[10]
Amberlite CG-400 112.36 mg/g for U	[40]
Dowex 2 × 8 303.03 mmol/g for U	[41]
Amberlyst A27 14.6 mg/g for U	[42]
AXAD-16-POPDE polymer U 1.38 and Th 1.33 mmol/g	[43]
XAD-16 functionalized with (bis-3,4-dihydroxy benzyl)p-phenylene diamine U 1.43 and Th 1.19 mmol/g	[44]

DOI: https://doi.org/10.35702/nano.10020

ISSN: 2767-0171

XAD-4 functionalized with succinic acid 12.3 mg/g for U	[15]
Ambersep 920 U (Cl-) 50 mg/g for U	[45]
Chitosan stearoyl thiourea 98.75 mg/g for U	[46]
Pyridylazo resorcinol—functionalized Amberlite XAD-16 115.5 mg/g for U	[47]
potato peels waste adsorpant without treatment 19.25 mg/g for U	[48]
The impregnation of Cyanex 921 into Amberlite XAD-4 U 333.3 and Th 434.7 mg/g	This study

Elution Studies

An amount of adsorbent was subjected to the optimum factors to adsorb uranium and thorium. Additionally, desorption experiments of uranium are well-performed in a batch mode. The quantitative desorption of U(VI) and Th(IV) was performed with various eluting agents, such as hydrochloric acid, nitric acid, ammonium carbonate and sulfuric acid, which form stable complexes with uranium and thorium [49,50]. For this purpose, 10 mL aliquots of each eluting agent with various concentrations were treated with 0.1 g portions of loaded impregnated resin at 25 °C for 30 min. From Table 6, we can conclude that the maximum elution efficiency (92.5%) of uranium was achieved by 2 M nitric acid, while the maximum elution efficiency (95.3%) of thorium was achieved by 2M hydrochloric acid. Results obtained indicate that the two cations can be well-separated from each other, especially at high HCl concentrations where the uranium uptake percent is quantitative and the thorium uptake is generally zero. From these results the selective elution of uranium over thorium was achieved. The excellent regeneration and reusability of modified resin indicated that it is a favorable applicant for effective radionuclides sorption from a large volume of aqueous solution.

Table 6. Effect of different eluting agents on uranium and thorium elution efficiency from loaded impregnated resin at 25 °C for 30 min

Eluting Agent / (%E)	U (VI)	Th (IV)
HCl	70.1	95.3
H_2SO_4	81.4	85.2
HNO_3	92.5	80.4
$NH_4(CO_3)_2$	40.7	48.09

CASE STUDY

A technological sedimentary lower carbonaceous sandstone rock sample collected from Southwestern Sinai, Egypt, was the studied sample for an experiment of the impregnated resin on a real sample. It was crushed, ground to −200 mesh size and quartered for complete analysis for major oxides, trace elements, uranium and gold. A scanning electron microscope (SEM) revealed the presence of micro-sized grains of gold and uranothorite, a radioactive material [51]. The total REE, U, Th, As and Cu were analyzed using ICP-MS in Achme Laboratories, Canada, while the gold was analyzed and monitored throughout the whole experiment using a studied, developed, gold-determining procedure using AAS [52], and the concentration of gold in the rock sample was confirmed using the well-known fire assay method in the Egyptian Geological Survey Laboratories. An atomic absorption spectrometer model, Unicam 969, supplied with acetylene and nitrous oxide burner heads was used for the analysis of gold after extraction with MIBK and stripping from the leach liquor.

ISSN: 2767-0171

The fire assay analysis of gold assured the presence of economic concentrations of 5 ppm gold and 160 ppm uranium analyzed volumetrically by the known Davies and Gray method [53]. Chemical analyses of major and trace concentrations in the studied sample are shown in Table 7 [54].

Table 7. Chemical composition of the working sedimentary lower carbonaceous sandstone rock sample

Oxide	Concentration (%)	Trace Elements	Concentration (ppm)
SiO_2	71.0	Au	5.0
Al_2O_3	5.30	Ag	10.0
Na_2O	0.60	U	160
K_2O	0.27	Th	8.60
CaO	3.10	ΣREEs	513
MgO	0.92	Cu	128
TiO_3	0.04	As	125
P_2O_5	0.86		
Fe_2O3	8.48		
L.O.I	6.80		

Take 5 g of the rock sample, opened by solution A, and take 10 mL of the solution, adapted with a pH of 3, batched with 0.01 g of the resin for 30 min. The SEM and EDX are presented in Figure 13 as the following:

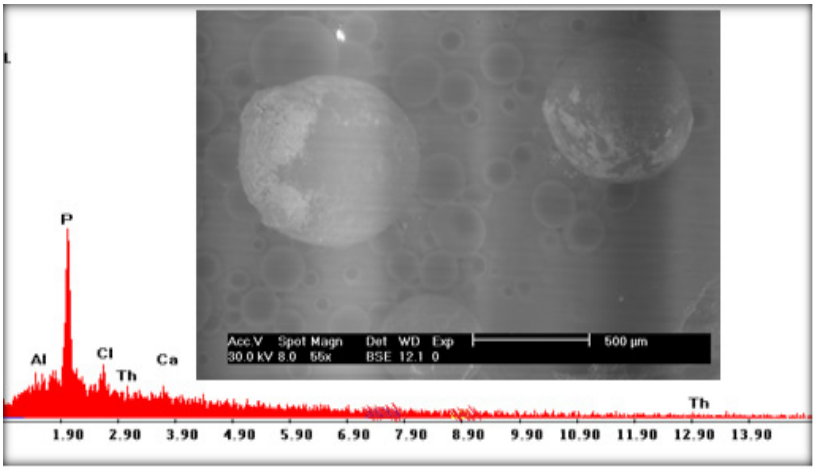

Figure 13. EDX and SEM images for impregnated Amberlite XAD-4 resin after thorium adsorption from the working sedimentary lower carbonaceous sandstone rock sample.

Adapt the solution with a pH of 4, batched with 0.01 g of the resin for 60 min. The SEM and EDX are shown in Figure 14 as the following:

DOI: https://doi.org/10.35702/nano.10020

ISSN: 2767-0171

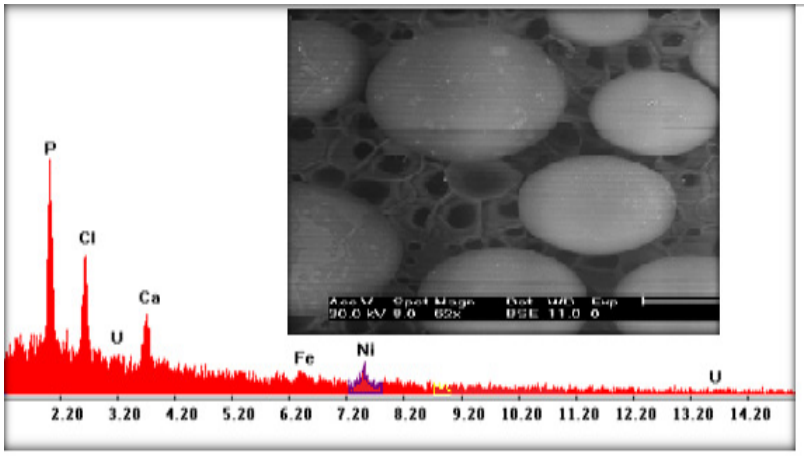

Figure 14. EDX and SEM images for impregnated Amberlite XAD-4 resin after uranium adsorption from the working sedimentary lower carbonaceous sandstone rock sample.

After applying the impregnated Amberlite XAD-4 resin to the lower carbonaceous sandstone rock sample collected from Southwestern Sinai, it was found that the resin was successful in the separation of thorium and uranium from the mentioned sample, as mentioned previously and shown in Figures 13 and 14. The impregnated Amberlite XAD-4 resin was applies also for REEs elements separation from acidified leach liquor of monazite mineral [21, 55].

CONCLUSIONS

The present work confirmed that uranium (VI) and thorium (IV) adsorption onto impregnated Amberlite XAD-4 resin in the presence of sulphate anions is affected by different parameters (pH, adsorbent dosage, contact time, initial concentration and different temperatures). The adsorptions were rapid during the first 30 min, and reached equilibrium in 60 min, which occurred at a pH of 4 and 3 for uranium and thorium a, respectively. The adsorption kinetics can be well-described by the pseudo-second-order model, indicating that chemical adsorption was the rate-limiting step. Equilibrium studies have shown that the uranium and thorium adsorption process follows the Langmuir model, and that the maximum adsorption capacity obtained by the Langmuir equation is 333.33 and 434.78 mg/g for uranium and thorium, respectively. Uranium and thorium adsorption onto impregnated Amberlite resin in the presence of sulphate is an unfavorable process at higher levels of temperature during the experiments. Furthermore, it is an exothermic and spontaneous process. Finally, it can be concluded that Cyanex-921-based Amberlite XAD-4 impregnated resin as a recent technique promises a wide applicability for the separation and removal of different trace elements. U (VI) and Th (IV) are successfully extracted, to a great extent, from aqueous media of the working sedimentary lower carbonaceous sandstone rock sample by using Cyanex-921-impregnated resin.

FUNDING

This research received no external funding.

INSTITUTIONAL REVIEW BOARD STATEMENT

Not applicable.

INFORMED CONSENT STATEMENT

Not applicable.

DATA AVAILABILITY STATEMENT

The data presented in this study are available on request from the corresponding author.

CONFLICTS OF INTEREST

The authors declare no conflict of interest.

ISSN: 2767-0171

AUTHOR CONTRIBUTIONS

Soaad Mohamed Elashry and A.I. L. Abd El Fatah conception, design of the work, performed the experiments, data analysis and drafted the manuscript investigation, data curation, review and editing. Fatma S. Hassen performed some experimental works. All authors approved the manuscript.

REFERENCES

1. Elashry SM, Labib S, Attallah MF. (2022). Sorption behavior of natural uranium from aqueous solutions using modified acti-vated carbon with quinolone. Radiochim Acta. 110(3):157-171.

2. Depleted Uranium At Hawaiian Military Sites Schofield Barracks Impact Area Makua Military Reservation Pohakuloa Training Area On Islands Of Oahu And Hawaii U.S. Department Of Health And Human Services Public Health Service Agency for Toxic Substances and Disease Registry Division of Health Assessment and Consultation Atlanta, Georgia 30333, AUGUST 25, 2008.

3. Shen Y, Wang S, Zhu L, Wang J, Wu W. (2011). Extraction of Th(IV) from an HNO_3 solution by diglycolamide in ionic liquids. Ind Eng Chem Res. 50(24):13990-13996.

4. Humelnicu D, Bulgariu L, Macoveanu M. (2010). On the retention of uranyl and thorium ions from radioactive solution on peat moss. J Hazard Mater. 174(1-3):782-787.

5. Geckeler EK, Nalwa H. (2001). Functional Polymers for Metal Ion Complexation and Separation. Advanced Functional Molecules and Polymers; Gordon and Reach Science Publishers: Singapore. Volume 4.

6. Wang S, Zhang R. (2006). Column preconcentration of lead in aqueous solution with macroporous epoxy resin-based polymer monolithic matrix. Anal Chim Acta. 575(2):166-171.

7. Rao GPC, Veni SS, Pratap K, Rao YK, Seshaiah K. (2006). Solid phase extraction of trace metals in seawater using morpholine dithiocarbamate-loaded Amberlite XAD-4 and determination by ICP-AES. Anal Lett. 39(5):1009-1021.

8. Filik H. (2002). Metal ion preconcentration with amberlite XAD-2 functionalized with 5-palmitoyl-8-hydroxyquinoline and its analytical applications. Anal Lett. 35(5):881-894.

9. Lee CH, Suh MY, Joe KS, Eom TY, Lee W. (1997). A chelating resin containing 4-(2-thiazolylazo) resorcinol as the functional group. Chromatographic application to the preconcentration and separation of some trace metal ions including uranium. Anal Chim Acta. 351(1-3):57-63.

10. Dev, K.; Pathak, R.; Rao, G.N. Sorption behaviour of lanthanum(III), neodymium(III), terbium(III), thorium(IV) and uranium(VI) on Amberlite XAD-4 resin functionalized with bicine ligands. *Talanta* **1999**, *48*, 579–584.

11. Seyhan S, Merdivan M, Demirel N. (2008). Use of o-phenylene dioxydiacetic acid impregnated in Amberlite XAD resin for separation and preconcentration of uranium(VI) and thorium(IV). J Hazard Mater. 152(1):79-84.

12. Korkisch J. (1988). Handbook of Ion Exchange Resins: Their Application to Inorganic Analytical Chemistry; CRC: Boca Raton, FL, USA.

13. Bhatt KD, Vyas DJ, Gupte HS, Makwana BA, Darjee SM, Jain VK. (2014). Solid phase extraction, preconcentration and sequential separation of U(VI), Th(IV), La(III) and Ce(III) by Octa-O-methoxy resorcin [4]arene based Amberlite XAD-4 Chelating Resin. World J Anal Chem. 2(2):31-41.

14. Orabi AH, Elenein SA, Abdulmoteleb SS. (2019). Amberlite XAD-2010 Impregnated with Chrome Azurol S for Separation and Spectrophotometric Determination of Uranium and Thorium. Chem Afr. 2:673-688.

15. Metilda P, Sanghamitra K, Mary Gladis J, Naidu GR, Prasada Rao T. (2005). Amberlite XAD-4 functionalized with succinic acid for the solid phase extractive preconcentration and separation of uranium(VI). Talanta. 65(1):192-200.

16. Çekiç SD, Filik H, Apak R. (2004). Use of an *o*-aminobenzoic acid-functionalized XAD-4 copolymer resin for the separation and preconcentration of heavy metal(II) ions. Anal Chim Acta. 505(1):15-24.

ISSN: 2767-0171

17. Merdivan M, Düz MZ, Hamamci C. (2001). Sorption behaviour of uranium(VI) with N,N-dibutyl-N'-benzoylthiourea Impregnated in Amberlite XAD-16. Talanta. 55(3):639-645.

18. Kumar M, Rathore DPS, Singh AK. (2001). Pyrogallol immobilized Amberlite XAD-2; A newly designed collector for enrichment of metal ions prior to their determination by flame atomic absorption spectromety. Microchim Acta. 137:127-134.

19. Sid Kalal H, Panahi HA, Hoveidi H, Taghiof M, Menderjani MT. (2012). Synthesis and application of Amberlite xad-4 functionalized with alizarin red-s for preconcentration and adsorption of rhodium (III). Iranian J Environ Health Sci Eng. 9(1):7.

20. Hosseini MS, Hosseini-Bandegharaei A, Raissi H, Belador F. (2009). Sorption of Cr(VI) by Amberlite XAD-7 resin impregnated with brilliant green and its determination by quercetin as a selective spectrophotometric reagent. J Hazard Mater. 169(1-3):52-57.

21. A. I. L. Abd El Fatah, Elashry SM. (2022). La (III) Separation by tri octyl phosphine oxide (Cyanex 921) Based on Amberlite Xad-4 Chelating Resin. J Inorg Organomet Polym. DOI: 10.1007/s10904-022-2344-7

22. Nascimento MRL, Fatibello-Filho O, Teixeira LA. (2004). Recovery of uranium from acid mine drainage waters by ion exchange. Miner Process Extr Metall. 25(2):129-142.

23. Ladeira AC, Gonçalves CR. (2007). Influence of anionic species on uranium separation from acid mine water using strong base resins. J Hazard Mater. 148(3):499-504.

24. Li WJ, Tao ZY. (2002). Comparative study on Th(IV) sorption on alumina and silica from aqueous solutions. J Radioanal Nucl Chem. 254:187-192.

25. Ekberg C, Albinson Y, Comarmond MJ, Brown PL. (2000). Studies on the complexation behavior of thorium(IV). 1. Hydrolysis equilibria. J Solution Chem. 29:63-86.

26. Fan FL, Qin Z, Bai J, Rong WD, Fan FY, Tian W, et al. (2012). Rapid removal of uranium from aqueous solutions using magnetic Fe3O4@SiO2 composite particles. J Environ Radioact. 106:40-46.

27. Ho YS, McKay G. (1999). Pseudo-second order model for sorption processes. Process Biochem. 34(5):451-465.

28. Ho YS. (2006). Review of second-order models for adsorption systems. J Hazard Mater. 136(3):681-689.

29. Wu FC, Tseng RL, Juang RS. (2001). Enhanced abilities of highly swollen chitosan beads for color removal and tyrosinase immobilization. J Hazard Mater. 81(1-2):167-177.

30. Eleonora G, Antonio G, Stefano S. (2020). Modelling the Kinetics of Elements Release from a Zeolitic-Rich Tuff. Environments. 7(6):41.

31. Langmuir I. (1918). The adsorption of gases on plane surfaces of glass, mica and platinum. J Am Chem Soc. 40(9):1361-1403.

32. Freundlich HMF. (1906). Over the adsorption in solution. J Phys Chem. 57:385-471.

33. Webi TW, Chakravort RK. (1974). Pore and solid diffusion models for fixed-bed adsorbers. AIChE J. 20:228-238.

34. Khawassek YM, Eliwa AA, Haggag EA, Mohamed SA, Omar SA. (2017). Equilibrium, Kinetic and Thermodynamics of Uranium Adsorption by Ambersep 400 SO_4 Resin. Arab J Nucl Sci Appl. 50(4):100-112.

35. Riegel M, Schlitt V. (2017). Sorption dynamics of uranium onto anion exchangers. Water. 9(4):268.

36. Solgy M, Taghizadeh M, Ghoddocynejad D. (2015). Adsorption of uranium(VI) from sulphate solutions using Amberlite IRA-402 resin: Equilibrium, kinetics and thermodynamics study. Ann Nucl Energy. 75:132-138.

37. Hazer O, Kartal S. (2009). Synthesis of a novel chelating resin for the separation and preconcentration of uranium(VI) and its spectrophotometric determination. Anal Sci. 25(4):547-551.

38. Atia AA. (2005). Studies on the interaction of mercury(II) and uranyl(II) with modified chitosan resins. Hydrometallurgy. 80(1-2):13-22.

ISSN: 2767-0171

39. Elashry SM. (2018). Extraction of Uranium and Copper from Calcareous Shale, Um Bogma formation, G. Allouga, Southwestern Sinai, Egypt, Phd, faculty of science – Ain shams University.

40. Semnani F, Asadi Z, Samadfam M, Sepehrian H. (2012). Uranium (VI) sorption behavior onto Amberlite CG-400 anion exchange resin: Effects of pH, contact time, temperature and presence of phosphate. Ann Nucl Energy. 48:21-24.

41. Kosari M, Sepehrian H. (2016). Uranium removal from aqueous solution using ion-exchange resin DOWEXÂ® 2x8 in the presence of sulfate anions. Int J Eng. 29(12):1677-1683.

42. Massoud A, Masoud AM, Youssef WM. (2019). Sorption characteristics of uranium from sulfate leach liquor by commercial strong base anion exchange resins. J Radioanal Nucl Chem. 322(2):1065-1077.

43. Prabhakaran D, Subramanian MS. (2004). Extraction of U(VI), Th(IV), and La(III) from acidic streams and geological samples using AXAD-16-POPDE polymer. Anal Bioanal Chem. 380(3):578-585.

44. Prabhakaran D, Subramanian MS. (2003). Selective extraction and sequential separation of e and transition ions using AXAD-16-BTBED polymeric sorbent. React Funct Polym. 57:147-155.

45. Cheira MF, El-Didamony AM, Mahmoud KF, Atia BM. (2014). Equilibrium and kinetic characteristics of uranium recovery by the strong base Ambersep 920U Cl resin. IOSRJAC. 7:32-40.

46. Orabi A, Atrees M, Salem H. (2018). Selective preconcentration of uranium on chitosan Steroyl thiourea prior to its spectrophotometric determination. Sep Sci Technol. 53:2267-2283.

47. Cheira M. (2015). Synthesis of pyridylazo resorcinol—functionalized Amberlite XAD-16 and its characteristics for uranium recovery. J Environ Chem Eng. 3:642-652.

48. El Pasir AA, Roshdi RA, Salem HM, Abd El Fatah AIL. (2025). Removal of Uranium from aqueous solution Using Potato Peels as Bio-Sorbent. Journal of Research in Environmental and Earth Sciences. 11(6):70-83.

49. Hosseini-Bandegharaei A, Hosseini M, Jalalabadi Y, Nedaie M, Sarwghadi M, Taherian A, et al. (2011). A novel extractant impregnated resin containing carminic acid for selective separation and pre-concentration of uranium(VI) and thorium(IV). Int J Environ Anal Chem. 93(1):1-17.

50. Elsalamouny A, Desouky O, Mohamed S, Galhoum A. (2016). Evaluation of adsorption behavior for U(VI) and Th(IV) ions onto solidified Mannich type material. J Dispers Sci Technol. 38:860-865.

51. el Assy IE, Gabr MM, Ibrahim EM. (2015). Base and Rare Metals Bearing Lower Carbonaceous Sa]ndstone in Southwestern Sinai, Egypt. Egypt J Geol. 59:199-208.

52. Fouad RK, Elrakaiby RM, Hashim MD. (2015). The application of flame atomic absorption spectrometry for gold determination in some of its bearing rocks. Am J Anal Chem. 6(5):411-421.

53. Davies W, Gray W. (1964). A rapid specific titrimetric method for the precise determination of uranium using iron (II) sulphate as a reductant. Talanta. 11(8):1203-1211.

54. Hisham KF, Randa ME, Fatah AIAE, Mohamed DH. (2019). Selective Leaching for Uranium and Gold from their Bearing Sedimentary Lower Carbonaceous Sandstone Rocks, Southwestern Sinai, Egypt. J Pet Min Eng. 21(1):90-96.

55. A. I. L. Abd El Fatah. (2021). An Innovative Method for Egyptian Monazite Mineral Digestion by Sulfuric Acid. International Journal of Science and Research (IJSR). 10(3). DOI: 10.21275/SR21316221646.